Staggered grids discretization in three-dimensional Darcy convection

Karasözen B. [a] Nemtsev A. D. [b] , Tsybulin V. G. [b]

[a] *Department of Mathematics and Institute of Applied Mathematics, Middle East Technical University, Ankara, Turkey*

[b] *Department of Computational Mathematics, Southern Federal University, Rostov-on-Don, Russia*

Abstract

We consider three-dimensional convection of an incompressible fluid saturated in a parallelepiped with a porous medium. A mimetic finite-difference scheme for the Darcy convection problem in the primitive variables is developed. It consists of staggered nonuniform grids with five types of nodes, differencing and averaging operators on a two-nodes stencil. The nonlinear terms are approximated using special schemes. Two problems with different boundary conditions are considered to study scenarios of instability of the state of rest. Branching off of a continuous family of steady states was detected for the problem with zero heat fluxes on two opposite lateral planes.

Key words: convection, porous medium, Darcy law, cosymmetry, finite-differences, staggered grids, family of equilibria
PACS: 02.30.Jr, 02.70.Bf, 47.55.Mh

Introduction

Several algorithms (finite element, finite difference, finite volume and spectral methods) are used for the simulation of physical problems involving partial differential equations (PDEs). Usually, the PDEs express fundamental physical laws like conservation of mass, momentum and total energy. While solving such problems, some information about the problem and its structure is lost during the discretization that replaces the PDE by a system of algebraic equations. In recent years so-called mimetic discretizations were developed to yield

Email address: bulent@metu.edu.tr (Karasözen B.).

stable and accurate solutions by preserving the analytical properties of the underlying PDEs [1,2]. Several mimetic or conservative finite difference methods were derived and their conservation properties were discussed for PDEs arising in fluid dynamics [3,4,5]. Experience shows that discrete conservation of mass, momentum and kinetic energy produce better results as compared with nonconservative methods.

The main goal of this paper is to develop a mimetic scheme for three-dimensional equations of the convection in a porous medium. Natural convection of incompressible fluid in a porous medium differs from the convection of a single fluid [6]. Usually, after the state of rest loses its stability, a finite number of regimes (convective patterns) may appear. An exciting example with an infinite number of steady states was found for the planar problem of incompressible fluid convection in a porous medium based on the Darcy law [7]. This case of the appearance of a continuous family of equilibria was explained by the cosymmetry theory [8,9].

To compute a continuous family of steady states we need the numerical scheme to be mimetic of the underlying system. The approximation of the planar Darcy convection equations was done for the first time using the Galerkin method [10]. Then the computations of the families of steady states were performed using the finite-difference scheme [11,12] and a combination of spectral and finite-difference approaches [13]. In [14] a staggered grid discretization for the planar problem of Darcy convection was developed in primitive variables. Special approximation of the nonlinear terms of the underlying system was the crucial step in all these works. It was found that the loss of gyroscopic and cosymmetric properties in the finite-dimensional approximation destroys the family of steady states and leads to a finite number of isolated stationary regimes [11,13].

In this work we consider the three-dimensional problem of natural convection in a porous medium and develop a finite-difference scheme for a system in primitive variables (velocities, pressure and temperature). The discretization is based on nonuniform staggered grids [14] with five types of nodes by using the differencing and averaging operators on two-nodes stencil. The present finite difference scheme is constructed in the spirit of the fully conservative second-order finite difference scheme for incompressible flow on nonuniform grids [5]. An algorithm for the computation of the family of steady states is described, and is used in numerical computations.

This paper is organized as follows. The equations for the three-dimensional Darcy convection problem in primitive variables are formulated in Section 1. In Section 2, the grids, discrete operators and discretization in space are described. The computation of the continuous family of steady states with varying stability spectra (cosymmetric family) is described in Section 3. Nu-

merical results on the branching off of the family of steady states and isolated regimes from the state of rest are presented in Section 4.

1 Darcy convection

1.1 Darcy equations in primitive variables

We consider an enclosure filled by a porous medium saturated by an incompressible fluid which is heated from below. We assume that the fluid is incompressible according to the Boussinesq approximation [6]. The system of equations consists of the momentum equation based on the Darcy law

$$\frac{1}{\varepsilon}\dot{v} = -\nabla p + \theta\gamma - v, \tag{1}$$

and the continuity and energy equations

$$\nabla \cdot v = 0, \tag{2}$$

$$\dot{\theta} = \Delta\theta - \lambda v \cdot \gamma - (v \cdot \nabla)\theta. \tag{3}$$

Here $v = (v^1, v^2, v^3)^T$ is the velocity vector, $\gamma = (0, 0, -1)^T$ is the direction of gravity, $p(x, y, z, t)$ is the pressure, $\theta(x, y, z, t)$ is the deviation of the temperature from a linear (in z) profile, ϵ is the porosity of the medium, x, y, z are the space variables and the dot accent denotes differentiation w.r.t. time t.

The Rayleigh number is defined as $\lambda = \alpha g T K l/\chi\mu$, where α is the thermal expansion coefficient, g is the gravity acceleration, μ is the kinematic viscosity, χ is the thermal diffusivity of the fluid, K is the permeability coefficient, T is the characteristic temperature difference and l is the length parameter. We suppose that the temperature at the boundary is given by a linear function on the vertical coordinate z.

The parallelepiped $\mathcal{D} = [0, L_x] \times [0, L_y] \times [0, L_z]$, with length L_x, depth L_y and height L_z is filled with the fluid. The normal component of the velocity is equal to zero at the boundary

$$V \cdot n = 0, \quad (x, y, z) \in \partial\mathcal{D}. \tag{4}$$

We consider two problems with different boundary conditions for the temperature. The first problem is characterized by a temperature deviation θ equal

to zero at the boundary $\partial\mathcal{D}$ (Dirichlet boundary condition):

$$\theta = 0, \qquad (x, y, z) \in \partial\mathcal{D}. \tag{5}$$

The second problem has mixed boundary conditions: the heat flux equals zero on two lateral faces $\partial_1 D = \{y = 0\} \cup \{y = L_y\}$ and the temperature deviation θ is equal to zero on the remaining faces $\partial_2 D = D \setminus \partial_1 D$

$$\theta_y = 0, \quad (x, y, z) \in \partial_1 D, \quad \theta = 0, \quad (x, y, z) \in \partial_2 D. \tag{6}$$

The initial condition is given as follows

$$\theta(x, y, z, 0) = \theta_0(x, y, z), \quad v(x, y, z, 0) = v_0(x, y, z). \tag{7}$$

It is simple to check that the equations (1)–(5) are invariant with respect to the discrete symmetries

$$R_x : \{x, y, z, v^1, v^2, v^3, p, \theta\} \mapsto \{L_x - x, y, z, -v^1, v^2, v^3, p, \theta\}, \tag{8}$$
$$R_y : \{x, y, z, v^1, v^2, v^3, p, \theta\} \mapsto \{x, L_y - y, z, v^1, -v^2, v^3, p, \theta\}, \tag{9}$$
$$R_z : \{x, y, z, v^1, v^2, v^3, p, \theta\} \mapsto \{x, y, L_z - z, v^1, v^2, -v^3, p, -\theta\}. \tag{10}$$

This implies that with appropriate transformations of velocity, pressure and temperature deviation, a given set of solutions produces a new set.

1.2 Darcy equations for the temperature and stream function

When the initial velocity v_0 and the initial temperature distribution θ_0 do not depend on y the system (1)–(3), (5) has a two-dimensional solution

$$v^1 = v^1(x, z, t),\ v^2 = 0,\ v^3 = v^3(x, z, t),\ p = p(x, z, t),\ \theta = \theta(x, z, t). \tag{11}$$

In this case we can write our system as a system containing temperature and stream function. We follow the usual assumption in porous media flow and neglect inertia in the momentum equation. The continuity equation (2) is fulfilled automatically when the stream function ψ is given by

$$v^1 = -\psi_z, \quad v^3 = \psi_x. \tag{12}$$

Then the underlying system can be transformed to a new form. After application of the *curl*-operator to (1) we deduce

$$0 = \Delta_2\psi - \theta_x \equiv G, \quad \Delta_2() = ()_{xx} + ()_{zz}, \tag{13}$$

and using (12) we obtain from (3)

$$\dot{\theta} = \Delta_2\theta + \lambda\psi_x + J(\theta,\psi) \equiv F, \quad J(\theta,\psi) = \theta_x\psi_z - \theta_z\psi_x. \tag{14}$$

The boundary conditions for the system (13), (14) follow from (6):

$$\psi = \theta = 0, \quad (x,z) \in \partial\widehat{\mathcal{D}}, \text{ where } \widehat{\mathcal{D}} = [0,L_x] \times [0,L_z]. \tag{15}$$

and the initial condition is formulated only for the temperature

$$\theta(x,z,0) = \theta_0(x,z), \tag{16}$$

where θ_0 denotes the initial temperature distribution. For a given θ_0, the stream function ψ can be obtained from (13) and (6) as the solution of the Dirichlet problem via Green's operator $\psi = G\theta_x$.

Equations (13)–(15) require that the equilibrium $\theta = \psi = 0$ (state of rest), be stable if $\lambda < \lambda_{11}$, where $\lambda_{nm} = (2\pi n/a)^2 + (2\pi m/b)^2$ $(m,n \in Z)$ are the eigenvalues for the corresponding spectral problem. It was shown in [9] that the first critical value λ_{11} has multiplicity two for any domain D. As a result, a continuous family of steady states appears [7,8].

The system (13)–(15) possesses the cosymmetry property [8]: a vector-function $(\theta, -\psi)$ being orthogonal to the right-hand side of (13) and (14) in L_2. Then, we obtain the cosymmetry condition in the following form

$$\int\limits_{\widehat{\mathcal{D}}} (F\psi - G\theta)dxdz = \int\limits_{\widehat{\mathcal{D}}} \left[\Delta\theta\psi - \Delta\psi\theta + \lambda\psi_x\psi + \theta_x\theta + J(\theta,\psi)\psi\right] dxdz = 0. \tag{17}$$

This can be checked directly using integration by parts and Green's formulae.

For the integration of equations (13)–(15) it is essential to provide a discrete version of the cosymmetry condition. In [11] a regular uniform mesh was used and both stream function and temperature were defined at the same nodes. The Jacobian approximation was based on the Arakawa scheme [15] and a number of one-parameter families of steady states were computed. It was also found that a violation of the cosymmetry property led to a degeneration of the family. The application of staggered nonuniform grids for the problem (13)–(16) was considered in [14].

2 Spatial discretization

We have discretized the equations (1)–(7) using five different types of nodes: one for the pressure, another for the temperature and three nodes for the components of the velocity vector, see Fig. 1.

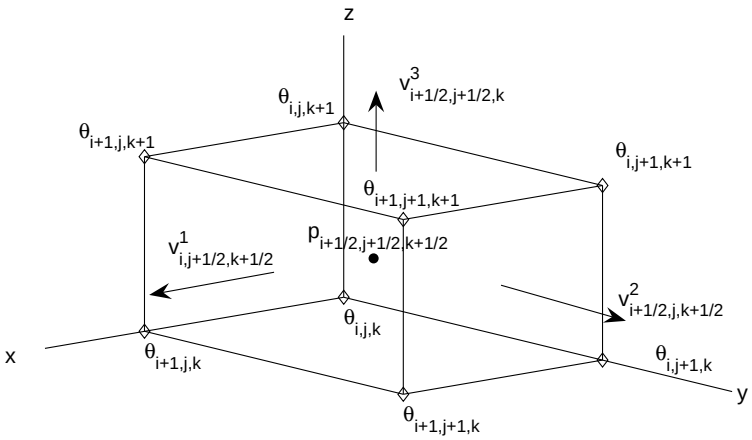

Fig. 1. Grid and nodes

For the first problem with Dirichlet boundary conditions (4) and (5) we introduce a nonuniform grid for the temperature θ

$$
\begin{aligned}
&0 = x_0 < x_1 < \ldots < x_{N_x+1} = L_x,\\
&0 = y_0 < y_1 < \ldots < y_{N_y+1} = L_y,\\
&0 = z_0 < z_1 < \ldots < z_{N_z+1} = L_z.
\end{aligned}
$$

The grid for the second problem with mixed boundary conditions (4) and (6) differs only in y direction

$$y_0 + y_1 = 0, \quad y_1 < \ldots < y_{N_y}, \quad y_{N_y} + y_{N_y+1} = 2L_y.$$

Thus the temperature θ is defined at the nodes

$$\omega_0 = \{(x_i, y_j, z_k),\, i = 0, \ldots, N_x + 1,\, j = 0, \ldots, N_y + 1,\, k = 0, \ldots, N_z + 1\}.$$

We introduce then the staggered grids along all coordinates

$$x_{i+1/2} = \frac{1}{2}(x_i + x_{i+1}), \quad i = 0, \ldots, N_x,$$
$$y_{j+1/2} = \frac{1}{2}(y_j + y_{j+1}), \quad j = 0, \ldots, N_y,$$
$$z_{k+1/2} = \frac{1}{2}(z_k + z_{k+1}), \quad k = 0, \ldots, N_z.$$

The velocities v^1, v^2 and v^3 are defined on the grids which are staggered respectively along the corresponding coordinates

$$\omega_1 = \{(x_i, y_{j+1/2}, z_{k+1/2}),\ i = 0, \ldots, N_x + 1,\ j = 0, \ldots, N_y,\ k = 0, \ldots, N_z\},$$
$$\omega_2 = \{(x_{i+1/2}, y_j, z_{k+1/2}),\ i = 0, \ldots, N_x,\ j = 0, \ldots, N_y + 1,\ k = 0, \ldots, N_z\},$$
$$\omega_3 = \{(x_{i+1/2}, y_{j+1/2}, z_k),\ i = 0, \ldots, N_x,\ j = 0, \ldots, N_y,\ k = 0, \ldots, N_z + 1\}.$$

Finally, the pressure p is defined at the nodes

$$\omega_p = \{(x_{i+1/2}, y_{j+1/2}, z_{k+1/2}),\ i = 0, \ldots, N_x,\ j = 0, \ldots, N_y,\ k = 0, \ldots, N_z\}.$$

In the case of Dirichlet boundary conditions we do not need any fictitious nodes for the discretization. In the case of mixed boundary conditions the grids are introduced in such a way that on $\partial_2 D$ the boundary conditions for the temperature and the normal component of velocity are fulfilled automatically. We define fictitious nodes for the temperature and velocity v^2 to approximate the boundary conditions on $\partial_1 D$.

2.1 Discrete finite-difference operators

To approximate (1)–(7) we define a set of discrete analogs of first order differential operators on a two-point stencil

$$\begin{aligned} d_1\theta_{i+1/2,j,k} &= \frac{\theta_{i+1,j,k} - \theta_{i,j,k}}{x_{i+1} - x_j} \approx (\theta_x)_{i+1/2,j,k}, \\ d_2\theta_{i,j+1/2,k} &= \frac{\theta_{i,j+1,k} - \theta_{i,j,k}}{y_{j+1} - y_j} \approx (\theta_y)_{i,j+1/2,k}, \\ d_3\theta_{i,j,k+1/2} &= \frac{\theta_{i,j,k+1} - \theta_{i,j,k}}{z_{k+1} - z_k} \approx (\theta_z)_{i,j,k+1/2}, \end{aligned} \tag{18}$$

and weighted averaging operators on the coordinates

$$\delta_1\theta_{i+1/2,j,k} = \frac{(x_{i+1} - x_{i+1/2})\theta_{i+1,j,k} + (x_{i+1/2} - x_i)\theta_{i,j,k}}{x_{i+1} - x_i} \approx (\theta)_{i+1/2,j,k},$$

$$\delta_2\theta_{i,j+1/2,k} = \frac{(y_{j+1} - y_{j+1/2})\theta_{i,j+1,k} + (y_{j+1/2} - y_j)\theta_{i,j,k}}{y_{j+1} - y_j} \approx (\theta)_{i,j+1/2,k}, \quad (19)$$
$$\delta_3\theta_{i,j,k+1/2} = \frac{(z_{k+1} - z_{k+1/2})\theta_{i,j,k+1} + (z_{k+1/2} - z_k)\theta_{i,j,k}}{z_{k+1} - z_k} \approx (\theta)_{i,j,k+1/2}.$$

The formulas (18)–(19) are valid both for integer and half-integer values of i, j and k. Then the discrete analog of the Laplacian on the seven-nodes stencil can be written as

$$\triangle_h = d_1 d_1 + d_2 d_2 + d_3 d_3 \approx \triangle, \quad (20)$$

and the averaging operator on three-dimensional cell is given as

$$\delta_0 = \delta_1\delta_2\delta_3. \quad (21)$$

The nonlinear term approximation is constructed using a linear combination of two terms

$$\begin{aligned}(v \cdot \nabla\theta)_{i,j,k} \approx J(\theta, v)_{i,j,k} = \quad (22)\\ = \frac{1}{3}\left[d_1\delta_1(\theta\delta_2\delta_3 v^1) + d_2\delta_2(\theta\delta_1\delta_3 v^2) + d_3\delta_3(\theta\delta_1\delta_2 v^3)\right]_{i,j,k}\\ + \frac{2}{3}\left[d_1\delta_2\delta_3(\delta_0\theta\delta_1 v^1) + d_2\delta_1\delta_3(\delta_0\theta\delta_2 v^2) + d_3\delta_1\delta_2(\delta_0\theta\delta_3 v^3)\right]_{i,j,k}.\end{aligned}$$

This provides second order accuracy for the uniform grid and an asymptotically second order accuracy for the quasi-uniform mesh. It allows conservation of energy and constitute a mimetic discretization of the underlying problem.

2.2 Semi-discretization

To reach some steady state it is useful to apply an approach based on artificial compressibility [16,17]. Thus instead of equation (2) we consider the following equation with coefficient η

$$\dot{p} + \frac{1}{\eta}\nabla \cdot v = 0. \quad (23)$$

Using the operators (18)–(22) we discretize system (1), (3) and (23) in the following form

$$\left[\dot{\theta} - \triangle_h\theta - \lambda\delta_1\delta_2 v^3 + J(\theta, v)\right]_{i,j,k} = 0, \quad (24)$$

$$\left[\dot{v^1} - \varepsilon(-d_1 p - v^1)\right]_{i,j+1/2,k+1/2} = 0, \tag{25}$$

$$\left[\dot{v^2} - \varepsilon(-d_2 p - v^2)\right]_{i+1/2,j,k+1/2} = 0, \tag{26}$$

$$\left[\dot{v^3} - \varepsilon(-d_3 p - v^3 + \delta_1\delta_2\theta)\right]_{i+1/2,j+1/2,k} = 0, \tag{27}$$

$$\left[\dot{p} + \frac{1}{\eta}(d_1 v^1 + d_2 v^2 + d_3 v^3)\right]_{i+1/2,j+1/2,k+1/2} = 0. \tag{28}$$

For the problem with Dirichlet boundary conditions (1)–(5) the grids are introduced in such a way that the nodes for the transversal velocity are located on the wall. It allows us to fulfill the boundary conditions on a rigid wall (5) in a very simple way for each pair of planes:
for $x = 0$ $(i = 0)$ and $x = L_x$ $(i = N_x + 1)$ we have

$$\begin{aligned} &v^1_{i,j+1/2,k+1/2} = 0, \quad j = 0, \ldots, N_y, \quad k = 0, \ldots, N_z, \\ &\theta_{i,j,k} = 0, \quad j = 0, \ldots, N_y + 1, \quad k = 0, \ldots, N_z + 1, \end{aligned} \tag{29}$$

for $y = 0$ $(j = 0)$ and $y = L_y$ $(j = N_y + 1$)we have

$$\begin{aligned} &v^2_{i+1/2,j,k+1/2} = 0, \quad i = 0, \ldots, N_x, \quad k = 0, \ldots, N_z, \\ &\theta_{i,j,k} = 0, \quad i = 0, \ldots, N_x + 1, \quad k = 0, \ldots, N_z + 1, \end{aligned} \tag{30}$$

and for $z = 0$ $(k = 0)$ and $z = L_z$ $(k = N_z + 1)$ we have

$$\begin{aligned} &v^3_{i+1/2,j+1/2,k} = 0, \quad i = 0, \ldots, N_x, \quad j = 0, \ldots, N_y, \\ &\theta_{i,j,k} = 0, \quad i = 0, \ldots, N_x + 1, \quad j = 0, \ldots, N_y + 1. \end{aligned} \tag{31}$$

The problem with mixed boundary conditions (1)–(4) and (6) is discretized using fictitious nodes to satisfy the boundary conditions on the planes $y = 0$ and $y = L_y$. Thus instead of (30) we have

$$\begin{aligned} &v^2_{i+1/2,0,k+1/2} = -v^2_{i+1/2,1,k+1/2}, \quad i = 0, \ldots, N_x, \quad k = 0, \ldots, N_z, \\ &v^2_{i+1/2,N_y+1,k+1/2} = -v^2_{i+1/2,N_y,k+1/2}, \quad i = 0, \ldots, N_x, \quad k = 0, \ldots, N_z, \\ &\theta_{i,0,k} = \theta_{i,1,k}, \quad \theta_{i,N_y+1,k} = \theta_{i,N_y,k}, \quad i = 0, \ldots, N_x + 1, \quad k = 0, \ldots, N_z + 1. \end{aligned} \tag{32}$$

2.3 Discrete equations for the planar problem

The system of ordinary differential equations (24)–(28), (29), (31) and (32) has a solution such that $v^2_{i+1/2,j,k+1/2} = 0$ and the other variables are invariant

w.r.t. index j. Then, we can exclude equation (26) and consider the two-dimensional problem. Moreover, we can eliminate pressure and velocities and reformulate the system with the discrete stream function and temperature. Let's define the stream function ψ at the nodes ω_0 using difference operators (18)

$$(d_3\psi)_{i,k+1/2} = -v^1_{i,k+1/2}, \quad (d_1\psi)_{i+1/2,k} = v^3_{i+1/2,k}. \tag{33}$$

The discrete analog of the continuity equation (2) is automatically fulfilled by (33). After the substitution of (33) in (25) and (27) and the combination of the resulting formulas we can deduce the analog of (13) (inertia terms are omitted)

$$\left[\Delta_{2,h}\psi - D_x\theta\right]_{i,k} = 0. \tag{34}$$

Similarly we find from (24)

$$\dot{\theta}_{i,k} = \left[\Delta_{2,h}\theta + \lambda D_x\psi + \frac{1}{3}J_D + \frac{2}{3}J_d\right]_{i,k}. \tag{35}$$

Here $D_x = d_1\delta_1$, $D_z = d_3\delta_3$ are the first order differencing operators on three-nodes stencils. The Laplacian and Jacobian are approximated using

$$\begin{aligned} &\Delta_{2,h} = d_1d_1 + d_3d_3, \\ &J_D = D_x\left(\theta D_y\psi\right) - D_y\left(\theta D_x\psi\right), \\ &J_d = \widehat{d_x}\left(\widehat{d_0}\theta\widehat{d_z}\psi\right) - \widehat{d_z}\left(\widehat{d_0}\theta\widehat{d_x}\psi\right), \end{aligned} \tag{36}$$

where $\widehat{d_0} = \delta_1\delta_3$, $\widehat{d_x} = d_1\delta_3$, $\widehat{d_z} = d_3\delta_1$.

The resulting scheme (34)–(36) ensures the fulfillment of a discrete analog of the cosymmetry property (17) as well as the nullification of the gyroscopic terms [12]. Equations in [11] follow from (34)–(36) for the case of the uniform grid $x_i = ih$, $z_k = kg$, $h = L_x/(N_x+1)$, $g = L_z/(N_z+1)$. Then the Jacobian approximation gives the famous Arakawa formula [15] on uniform grids $h = g$.

3 Computation of the family of steady states

We rewrite the resulting system of equations in vector form. Let us introduce vectors which contain only unknowns at internal nodes

$$\Theta = (\theta_{1,1,1}, \dots, \theta_{N_x,1,1}, \theta_{1,2,1}, \dots, \theta_{N_x,N_y,N_z}),$$
$$V^1 = (v^1_{1,1/2,1/2}, \dots, v^1_{N_x,1/2,1/2}, v^1_{1,3/2,1/2}, \dots, v^1_{N_x,N_y+1/2,N_z+1/2}),$$
$$V^2 = (v^2_{1/2,1,1/2}, \dots, v^2_{N_x+1/2,1,1/2}, v^2_{1/2,2,1/2}, \dots, v^2_{N_x+1/2,N_y,N_z+1/2}),$$
$$V^3 = (v^3_{1/2,1/2,1}, \dots, v^3_{N_x+1/2,1/2,1}, v^3_{1/2,3/2,1}, \dots, v^3_{N_x+1/2,N_y+1/2,N_z}),$$
$$P = (p_{1/2,1/2,1/2}, \dots, p_{N_x+1/2,1/2,1/2}, p_{1/2,3/2,1/2}, \dots, p_{N_x+1/2,N_y+1/2,N_z+1/2}),$$

and obtain the system which corresponds (24)–(28)

$$\begin{aligned}
&\dot{\Theta} = A_1\Theta + \lambda C_1 V^3 - F(\Theta, V),\\
&\dot{V^1} = -B_4 P - C_2 V^1,\\
&\dot{V^2} = -B_5 P - C_3 V^2,\\
&\dot{V^3} = -B_6 P - C_4 V^3 + C_5\Theta,\\
&\dot{P} = -B_1 V^1 - B_2 V^2 - B_3 V^3.
\end{aligned} \tag{37}$$

Here the matrices B_k, $k = 1, \dots, 6$, are constructed by the application of first order difference operators, and the matrices C_k, $k = 1, \dots, 5$, by the averaging operators. The matrix A_1 presents the discrete form of the Laplacian. The nonlinear term is given by $F(\Theta, V)$. Equations (37) form a system of

$$5N_xN_yN_z + 3(N_xN_y + N_xN_z + N_y + N_z) + 2(N_x + N_y + N_z) + 1$$

unknowns.

From (37) at $J = 0$ we can derive the perturbation equations (σ is a decrement of linear growth) to analyze the stability of the state of rest

$$\sigma\Theta = A_1\Theta + \lambda C_1 V^3, \tag{38}$$
$$\sigma V^1 = -B_4 P - C_2 V^1, \tag{39}$$
$$\sigma V^2 = -B_5 P - C_3 V^2, \tag{40}$$
$$\sigma V^3 = -B_6 P - C_4 V^3 + C_5\Theta, \tag{41}$$
$$\sigma P = -B_1 V^1 - B_2 V^2 - B_3 V^3. \tag{42}$$

For the decrement $\sigma = 0$ we obtain the system from which we can determine the threshold value of the Rayleigh number corresponding to the monotonic loss of stability. We can express P, V^1, V^2 V^3 via Θ from (38)–(42) and obtain a system of $N_xN_yN_z$ equations for the unkown vector Θ. Substituting (39), (40) and (41) into (42) we deduce

$$A_1\Theta = \lambda C_1(C_5 - B_6 S)\Theta. \tag{43}$$

Here we find the vector $P = S\Theta$ from the system of linear algebraic equations

with rank deficiency 1

$$(B_1C_2^{-1}B_4 + B_2C_3^{-1}B_5 + B_3C_4^{-1}B_6)P = B_3C_4^{-1}C_5\Theta.$$

Since for an incompressible flow the pressure may differ by a constant we can exclude one component of P and respectively one equation.

To find an isolated convective pattern we apply the direct approach and integrate the system of ordinary differential equations (37) by the classical fourth order Runge-Kutta method up to convergence.

To compute a family of steady states we apply the technique based on the cosymmetric version of the implicit function theorem [18] and the algorithm developed in [10,11,19]. The zero equilibrium $V^1 = V^2 = V^3 = P = \Theta = 0$ is globally stable for $\lambda < \lambda_1$ where λ_1 is the minimal eigenvalue for spectral problem (43). When λ is slightly larger than λ_1, then all points of the family are stable [9]. Starting from the vicinity of unstable zero equilibrium we integrate the ordinary differential equations (37) up to a point Θ_0 close to some stable equilibrium on the family. Then we correct the point Θ_0 by the Newton method. To predict the next point on the family we determine the kernel of the linearization matrix (Jacobi matrix) at the point Θ_0 and then use the Adams-Bashford method. This procedure is repeated to obtain the entire family of steady states. It is important to note that the given procedure allows us to compute the stable regimes as well as unstable ones.

4 Numerical results

V. Yudovich [8] proved that the appearance of a family of steady states in the planar Darcy convection is caused by the nontrivial cosymmetry of the problem. Loss of stability of the state of rest is characterized by the repeated eigenvalues for the corresponding spectral problem. For the problem under consideration we find the critical Rayleigh numbers from the system (43). There exist two scenarios of instability of the state of rest in the parallelepiped: branching off of isolated regimes and the appearance of a family of steady states [20]. In our computer experiment the emergence of the family was only observed for the problem with mixed boundary conditions. It was found that a family of stable equilibria has appeared in the case of rather small value of L_y/L_x (relative depth) which depends also on the ratio L_x/L_z.

It was shown in [14] that a uniform grid is the best choice for the computation of the critical Rayleigh numbers while a nonuniform grid is useful for the computation of a specific regime with a desirable accuracy. Thus, we use the uniform grids and set up the amount of internal nodes for the temperature as $N_x \times N_y \times N_z$.

4.1 Critical Rayleigh numbers

We present in Table 1 the first seven critical Rayleigh numbers λ for the problem with Dirichlet boundary conditions for several values of the depth L_y and fixed length $L_x = 2$ and height $L_z = 1$. In the case $L_y < 1$ ($L_y > 1$) the computation of critical Rayleigh numbers was carried out on the mesh of $14 \times 6 \times 6$ ($14 \times 10 \times 6$) internal nodes for the temperature.

Table 1
Dependence of critical Rayleigh numbers on the depth L_y for the problem with Dirichlet boundary conditions; $L_x = 2$, $L_z = 1$, mesh $14 \times 6 \times 6$ ($14 \times 10 \times 6$)

L_y	0.4	0.6	0.8	1.2	1.6
λ_1	157.5	99.2	77.9	62.0 (59.1)	(53.5)
λ_2	159.0	100.1	78.0	62.3 (59.7)	(54.9)
λ_3	207.0	138.4	108.5	83.4 (73.3)	(60.6)
λ_4	209.4	139.6	116.0	85.1 (78.2)	(66.0)
λ_5	298.3	178.7	122.9	90.0 (79.6)	(69.5)
λ_6	303.8	191.1	132.4	100.1 (95.2)	(81.4)
λ_7	310.5	192.0	152.1	107.6 (95.3)	(86.9)

One can see that some critical values in Table 1 are close to each other. When we take $L_x = L_y$ we find that some critical values coincide. For example, for $D = [0, 2] \times [0, 2] \times [0, 1]$ and the mesh $12 \times 12 \times 6$ we find that $\lambda_1 = 51.3$ and $\lambda_2 = \lambda_3 = 53.8$. But this is a consequence of the discrete symmetries on the x_1 and x_2 coordinates and doesn't lead to the appearance of a family of steady states.

We summarize in Table 2 the first seven critical Rayleigh numbers λ for the mixed boundary conditions problem for several values of the depth L_y and fixed length $L_x = 2$ and height $L_z = 1$. One can see that for $L_y = 0.4$ and $L_y = 0.6$ two minimal eigenvalues of the problem (43) are repeated. This corresponds to the birth of the continuous family of steady states. The parallelepiped with $L_y = 0.8$ gives a single minimal eigenvalue and that results in the appearance of two isolated stationary regimes.

Table 2
Dependence of critical Rayleigh numbers on the depth L_y for the problem with mixed boundary conditions; $L_x = 2$, $L_z = 1$, mesh $14 \times 6 \times 6$ ($14 \times 10 \times 6$)

L_y	0.4	0.6	0.8	1.2	1.6
λ_1	52.5	52.5	46.7	44.5 (42.5)	(45.7)
λ_2	52.5	52.5	52.5	51.6 (49.4)	(46.1)
λ_3	90.8	56.6	52.5	52.5 (52.5)	(49.6)
λ_4	93.1	66.8	56.2	52.5 (52.5)	(52.5)
λ_5	93.1	84.7	73.2	67.8 (58.1)	(52.5)
λ_6	102.1	93.1	93.1	68.3 (64.8)	(57.8)
λ_7	122.2	93.1	93.1	80.9 (68.6)	(66.3)

It should be noted that on the fixed mesh the threshold corresponding to the branching off of the family of steady states (repeated critical values) doesn't depend on the depth L_y. Comparison with results on the mesh $24 \times 6 \times 12$ shows that even a rough mesh allows to find a threshold (minimum of critical Rayleigh numbers) with accuracy about 10%. For instance, using the mesh $24 \times 6 \times 12$ we obtain $\lambda_1 = 50.5$ for $L_y = 0.4$ and $L_y = 0.6$ and $\lambda_1 = 46.8$ for $L_y = 0.8$.

On the other hand convection in a three-dimensional box with insulating impermeable lateral boundaries (the lateral walls are taken as thermally insulating) was a subject of numerous works [6]. We may refer here to [21] where it was shown that different two-dimensional and three-dimensional states appear depending on the initial conditions.

4.2 Computation of steady states

Now we study the mixed boundary conditions problem and consider the parallelepipeds with small depth when the family of stationary solutions branches off. The steady states belonging to the family are essentially two-dimensional and don't depend on the coordinate y.

Fig. 2 demonstrates this by the presentation of several convective patterns from the family: none has transversal motion to the plane $y = const$. The relative location of each steady state is given in Fig. 3 where each letter corresponds to a flow pattern in Fig. 2. In Fig. 3 we use the Nusselt values for

the planar problem [10]

$$Nu_v = \int_0^{L_z} \theta_x(\frac{L_x}{2}, 0, z)dz, \quad Nu_h = \int_0^{L_x} \theta_z(x, 0, 0)dx. \tag{44}$$

Here Nu_v corresponds to the cumulative heat flux from left to right defined for the centered vertical section of the rectangular domain. The value Nu_h is a combined heat flux through the bottom of the enclosure, $y = 0$.

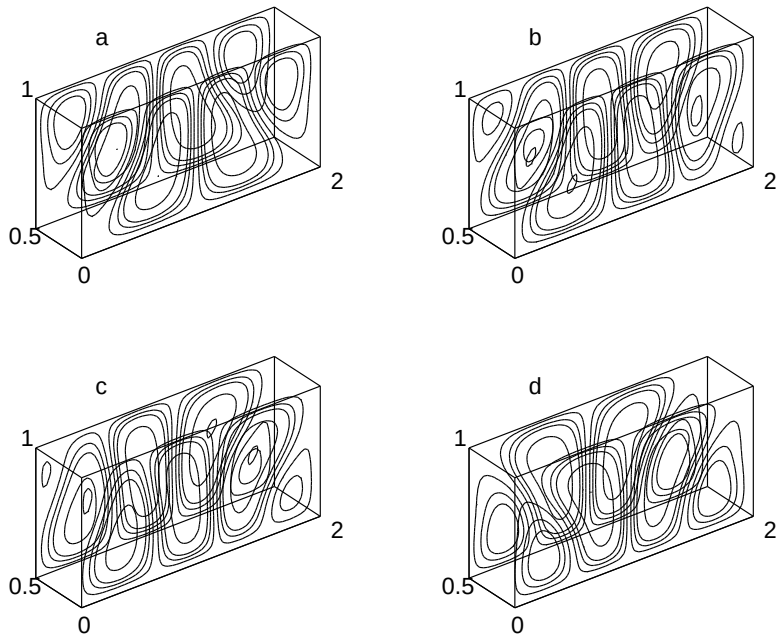

Fig. 2. Members of the family of steady states; $\lambda = 60$, $D = [0, 2] \times [0, 0.5] \times [0, 1]$

The regimes in Fig. 2 are the members of the family of steady states, because stability spectra for each state have exactly one value being zero with reliable accuracy (10^{-8}). We plot the distribution of eigenvalues of the Jacobi matrix (matrix of linearization) computed for the convective pattern with two symmetrical rolls (regime a in Fig. 3). We take different values of the depth L_y to demonstrate the three-dimensional instability on the family, see Fig. 4). It is clearly seen that exactly one point σ lies on the imaginary axis. The corresponding eigenvector defines the neutral direction along the family. Such a family is called cosymmetric, the stability of its members is governed by nonzero eigenvalues or defined on the submanifold being transversal to the family.

It should be noted that the given Rayleigh number is rather far from the

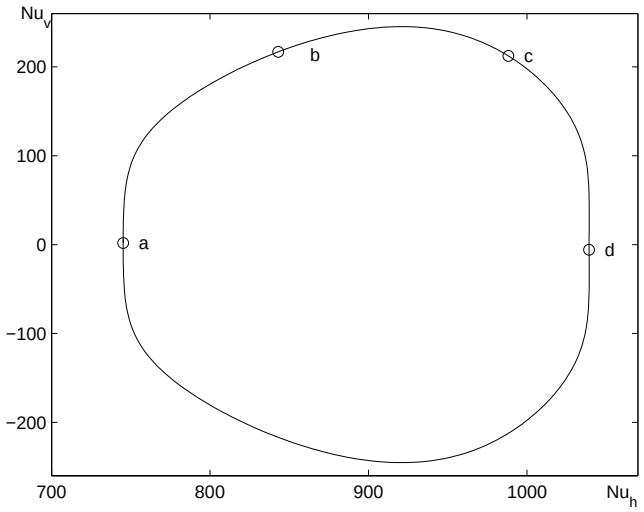

Fig. 3. Family of steady states; $\lambda = 60$, $D = [0, 2] \times [0, 0.5] \times [0, 1]$

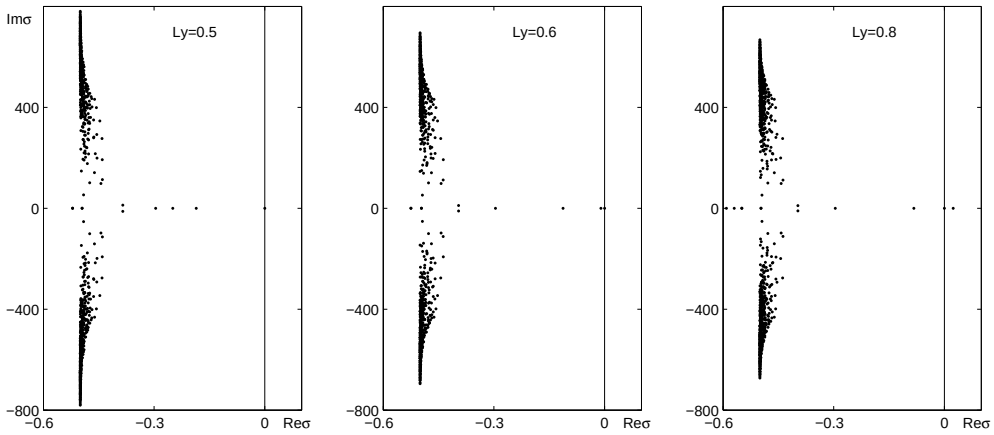

Fig. 4. Stability spectrum for the two-rolls steady state from the family; $\lambda = 100$, $L_x = 2$, $L_z = 1$

critical value when some members of the family become unstable. In the case of the parallelepiped $D = [0, 2] \times [0, 0.5] \times [0, 1]$ the family of steady states appears at $\lambda \approx 51$. The transformation of stability spectra with increasing λ is presented in Fig. 5. One can see that the symmetrical convective pattern lost its stability before $\lambda = 200$. Some states on the family become unstable at $\lambda \approx 190$. This value is less than $\lambda \approx 400$ which corresponds to the critical value of instability for the planar problem.

We present in Fig. 6 the distribution of spectra for different values of the depth L_y. One can see that the steady state with two rolls is stable when $L_y = 0.3$ and unstable for $L_y \geq 0.4$ (two spectra values in right part of the complex plane). When the Rayleigh number becomes greater the instability

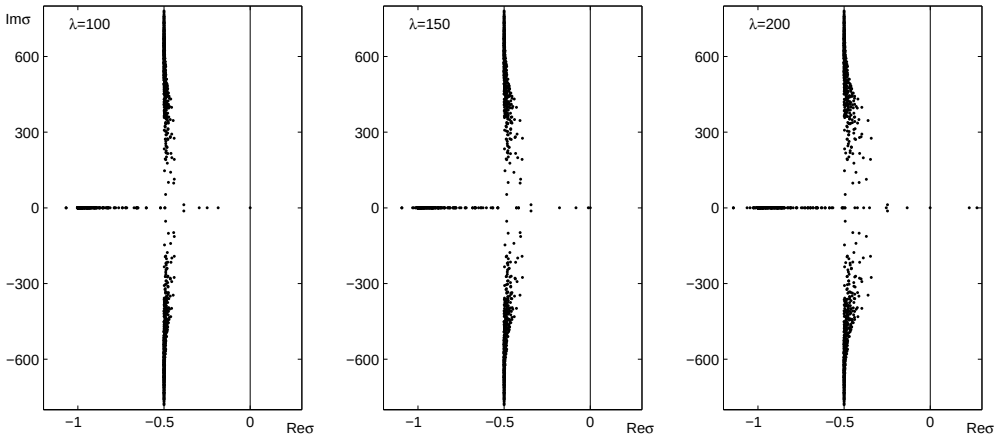

Fig. 5. Stability spectrum for symmetric two-rolls pattern from the family for different λ; $D = [0, 2] \times [0, 0.5] \times [0, 1]$

on the family occurs for smaller values of the depth L_y.

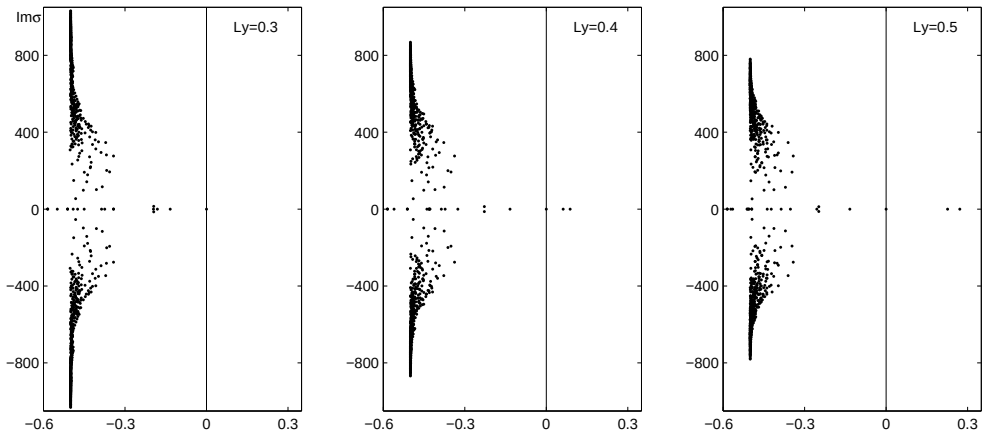

Fig. 6. Stability spectrum for the two-rolls steady state from the family; $\lambda = 200$, $L_x = 2$, $L_z = 1$

When the depth $L_y = 0.9$ the only isolated stable regimes are branched off of the state of rest. Because of the discrete symmetries of the problem (8)–(10) we obtained two regimes. The flow pattern for one of these regimes is presented in Fig. 7. The distribution of eigenvalues for this stable steady state is displayed in Fig. 8. One can see that the distribution of the stability spectra has no point close to the imaginary axis. This regime is essentially three-dimensional and isolated. Branching off the isolated convective regimes is characteristic for the parallelepipeds with non-small depth.

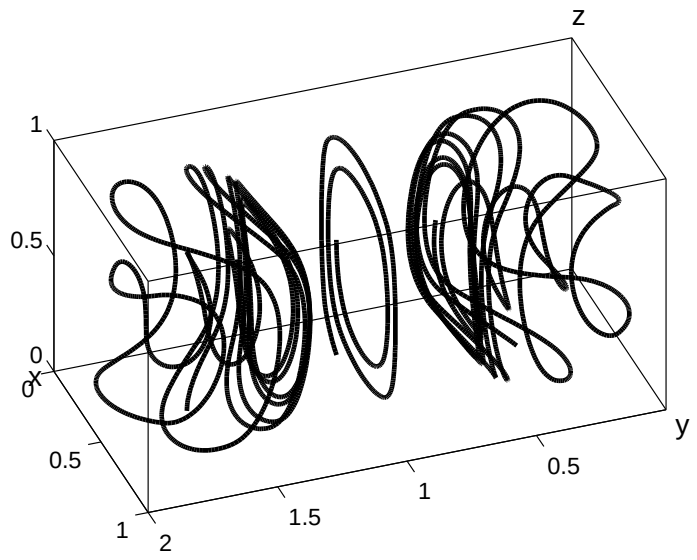

Fig. 7. Isolated steady state; $\lambda = 52$, $D = [0, 2] \times [0, 0.9] \times [0, 1]$

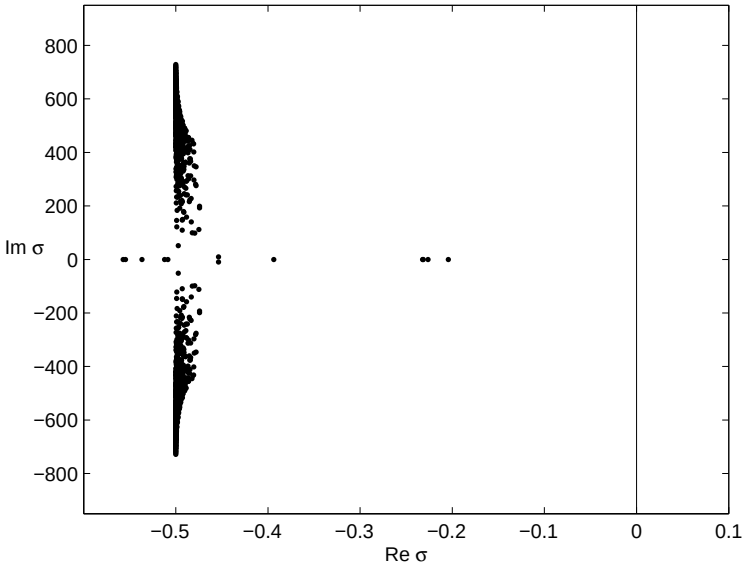

Fig. 8. Stability spectrum for the isolated steady state from the family; $\lambda = 52$, $D = [0, 2] \times [0, 0.9] \times [0, 1]$

5 Conclusion

Convection in a porous parallelepiped has demonstrated two different scenarios of instability of the state of rest. It was found by computer experiments that for zero heat fluxes on two lateral sides (mixed boundary conditions) the appearance of a cosymmetric continuous family of equilibria becomes possible.

To compute a continuous family of equilibria one needs to solve repeatedly a nonlinear system of algebraic equations that is degenerated in the vicinity of the family. This is why discretization is so important for the Darcy convection. We have developed the approach based on primitive variables equations and a finite-difference discretization with staggered nonuniform grids. This scheme mimics the nontrivial characteristics of the underlying problem that admits existence of a continuous family of steady states.

Acknowledgements

The authors thank to the referee for careful reading and advises. The authors acknowledge the support of Guest Researcher Fellowship Programme of TÜBITAK (Turkish Scientific Research Council). A.N. and V.T. were partially supported by the Program for the leading scientific schools (# 5747.2006.1) and Russian Foundation for Basic Research (# 08-01-00734) and the Program for National Universities of Russia.

References

[1] J. M. Hyman, J. Morel, M. Shashkov and S. Steinberg, *Mimetic Finite Difference Methods for Diffusion Equations*, Comput. Geosciences, **6** (2002), 333–352.

[2] J. M. Hyman, P. B. Bochev, *Principles of Mimetic Discretizations of Differential Operators*, IMA Volumes in Mathematics and Its Applications, 142, (2006), 89-114

[3] Y. Morinishi, T. S. Lund, O. V. Vasilyev, P. Moin, *Fully Conservative Higher Order Finite Difference Schemes for Incompressible Flow,* J. Comput. Phys. **143** (1998) 90–124.

[4] O.V. Vasilyev, *High order finite difference schemes on non-uniform meshes with good conservation properties*, J. Comput. Phys. 57 (2000) 746761.

[5] F. E. Ham, F. S. Lien, and A. B. Strong, *A Fully Conservative Second-Order Finite Difference Scheme for Incompressible Flow on Nonuniform Grids,* J. Comput. Phys. **177** (2002) 117-133.

[6] D. A. Nield, A. Bejan, Convection in porous media. Springer-Verlag, New York, 1999, 546 p.

[7] D. V. Lyubimov, *On the convective flows in the porous medium heated from below*, J. Appl. Mech. Techn. Phys. **16** (1975), 257–261.

[8] V. I. Yudovich, *Cosymmetry, degeneracy of the solutions of operator equations, and the onset of filtrational convection*, Math. Notes **49** (1991), 540-545.

[9] V. I. Yudovich, *Secondary cycle of equilibria in a system with cosymmetry, its creation by bifurcation and impossibility of symmetric treatment of it*, Chaos **5** (1995), 402–441.

[10] V. N. Govorukhin, *Numerical simulation of the loss of stability for secondary steady regimes in the Darcy plane-convection problem*, Doklady Akademii Nauk **363** (1998), 806–808.

[11] B. Karasözen, V. G. Tsybulin, *Finite-difference approximation and cosymmetry conservation in filtration convection problem*, Physics Letters **A 262** (1999), 321–329.

[12] B. Karasözen, V. G. Tsybulin, *Cosymmetry preserving finite–difference methods for convection equations in a porous medium,* Appl. Num. Math. **55** (2005) 69–82.

[13] O. Yu. Kantur, V. G. Tsybulin, *A spectraldifference method for computing convective fluid motions in a porous medium and cosymmetry preservation*, Computational Mathematics and Mathematical Physics **42** (2002) 878–888.

[14] B. Karasözen, V. G. Tsybulin, *Mimetic discretization of two-dimensional Darcy convection,* Comm. Comput. Phys. **167** (2005) 203–213.

[15] A. Arakawa, *Computational design for long-term numerical integration of the Equations of Fluid Motion: two-dimensional incompressible flow. Part I*, J. Comput. Phys. **1** (1966), 119–143.

[16] A. J. Chorin, *A numerical method for solving incompressible viscous flow problems,* J. Comput. Phys. **2** (1967) 12–26.

[17] N. A. Vladimirova, B. G. Kuznetsov, N. N. Yanenko, *Computation of the plane problem for symmetrical flow of the plate by the viscous incompressible fluid,* In "Some problems of applied and computational mathematics", Novosibirsk, Nauka (1966) 186–192.

[18] V. I. Yudovich, *An implicit function theorem for cosymmetric equations*, Math. Notes **60** (1996), 235–238.

[19] V. N. Govorukhin, *Calculation of one-parameter families of stationary regimes in a cosymmetric case and analysis of plane filtrational convection problem*, Continuation methods in fluid dynamics (Aussois, 1998), Notes Numer. Fluid Mech., **74**, Vieweg, Braunschweig, 2000, 133–144.

[20] D. A. Bratsun, D. V. Lyubimov, V. S. Teplov, *Three-dimensional convective flows in a porous cylindrical enclosure*, In: "Hydrodynamics", Perm, 1998, No. 11, 58–77.

[21] J. M. Straus, G. Schubert, *Three-dimensional convection in a cubic box of fluid-saturated porous material,* J. Fluid Mech. **91** (1979) 155-165.

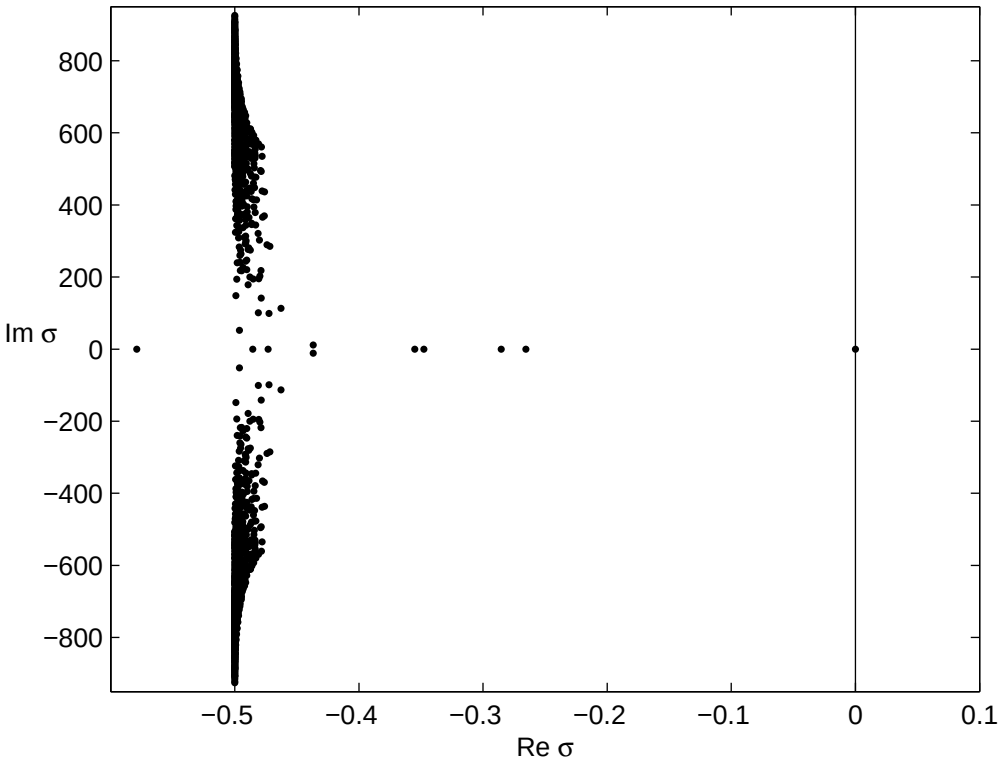
800
600
400
200
Im σ
0
−200
−400
−600
−800
−0.5
−0.4
−0.3
−0.2
−0.1
0
0.1
Re σ